Chaotic sound waves in a regular billiard

K. Schaadt,[1,2] A. P. B. Tufaile,[3] and C. Ellegaard[1]
[1]*Complexity Lab, Niels Bohr Institute, Blegdamsvej 17, 2100 Copenhagen Ø, Denmark*
[2]*CORE A/S, Lersøparkalle 42, 2100 Copenhagen Ø, Denmark*
[3]*Instituto de Fisica, Universidade de São Paulo, Caixa Postal 66318, 05315-970 São Paulo, Brazil*
(Received 1 September 2002; published 24 February 2003)

We present experimental results for the ultrasound transmission spectra and standing wave patterns of a rectangular block of fused quartz. A comparison is made between our data and an approximation of the theoretical staircase function for three-dimensional isotropic elasticity. The main emphasis of our study is on the role of mode conversion in regular ray-splitting billiards. We present the fluctuation statistics and find that these are described by the Gaussian orthogonal ensemble of random matrix theory, despite the fact that the system is not classically chaotic, as demonstrated with numerical simulation. Using temperature perturbation, we find that the vast majority of the resonances are mixtures of transverse and longitudinal wave motion, yet a small number of special resonances remain pure. We further illuminate this by presenting standing wave patterns measured on one face of the block.

DOI: 10.1103/PhysRevE.67.026213 PACS number(s): 05.45.Mt, 46.70.De, 62.30.+d

I. INTRODUCTION

Can you calculate the eigenfrequencies of a freely vibrating rectangular block of isotropic and homogeneous material? Confronted with this question, many physicists wrongly believe that the answer is positive. In fact, not even the exact average resonance density (Weyl formula) is known, much less the actual eigenfrequencies or the eigenfunctions. Renewed interest and insight in such classic problems of elastodynamics is now arising from the application of methods used in the field of quantum chaos.

It has been established [1] that the fluctuation properties of spectra from quantum billiards and from the flexing of thin plates are identical. This result was confirmed experimentally in Ref. [2], which also presented the theoretical Weyl formula and found agreement with the experimental result. Cavity scattering in elastodynamics has been investigated [3], and an important breakthrough occurred very recently when periodic orbits were used for the first time to calculate the level density for the elastic disc [4]. The rectangular plate was investigated experimentally [5] and an attempt to calculate the level density for this system, using periodic orbits, is under way [6].

The conjecture of Ref. [7] states that spectral fluctuations of quantum chaotic systems obey random matrix theory (RMT), and Ref. [8] states that also the motion of the energy levels of quantum chaotic systems, under a perturbation of an external parameter, obeys RMT. Experimental results with acoustic systems [9–13] strongly suggest the applicability of these two conjectures to a wider range of systems than quantum chaotic systems [14]. In that capacity, these experiments have served not just as analog systems of quantum billiards, but more generally, to promote problems of elastodynamics as interesting problems in their own right.

In this paper, we consider the free, resonant vibrations of a rectangular block of fused quartz. We are thus studying the three-dimensional version of the in-plane vibration modes of the rectangular plate, treated in Ref. [5]. For both of these systems, mode conversion is important: On the boundary, a purely transverse or purely longitudinal incoming wave is converted into two outgoing waves, one of each type, according to Snell's law [24]. Reference [15] found by numerical simulation of ray splitting in classical billiards that chaoticity is enhanced. Experimental studies of ray-splitting billiards have been carried out with modified Sinai microwave cavities, comparing results for the spectral fluctuations and parametric correlators to numerical calculations for the ray-splitting version of the annular billiard [16], and the triangular step billiard [17]. In Ref. [18] the spectra and wave functions of such experiments are given a semiclassical interpretation. These studies have all focused on ray-splitting systems that are classically chaotic. Here, we are interested in systems that are not classically chaotic, even when ray splitting is present. The rectangular plate is an example of such a system, and in Ref. [5] it was established experimentally that mode conversion gives rise to chaotic spectral fluctuations for this system. It is precisely this issue we now seek to clarify for the rectangular block.

We first present a comparison of the measured staircase function to an approximation including the two leading terms, first calculated by Dupuis, Mazo, and Onsager [19], then later by Safarov and Vassiliev [20]. We then present the fluctuation statistics of the resonances, in terms of the nearest neighbor spacing distribution and the $\Delta_3(L)$, and compare to random matrix results. To investigate the character of the resonances, we measure the distribution of normalized frequency shifts due to a temperature perturbation. This result can be directly compared to the corresponding result for the rectangular plate [5], but also serves as a guide for selection of resonances for which we measure the standing wave patterns by scanning one face of the block. One of the interesting aspects of our results is that we find both mixed states and states that are ''bouncing-ball''-like [21].

II. EXPERIMENTAL SETUP

We measure ultrasound transmission spectra of a rectangular block using piezoelectric transducers, see Fig. 1. There

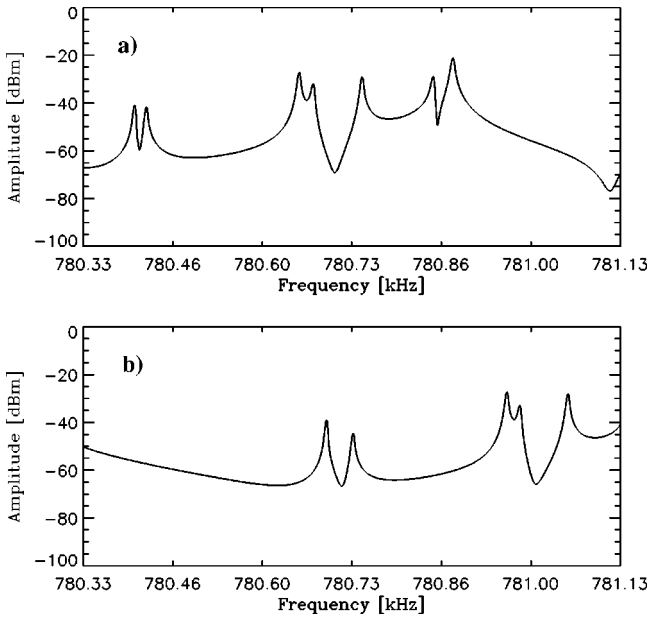

FIG. 1. Measured spectra at two different temperatures of the rectangular fused quartz block, 35 °C (a) and 40 °C (b).

are three such transducers, of which one is a transmitter and two are receivers. The temperature of the system is kept constant to within 0.005 °C using a temperature controller, such that the eigenfrequencies are not affected by fluctuations in room temperature. The pressure of the air surrounding the block can be controlled and kept at a low value where air damping of the block vibration is insignificant. During measurements, the block is resting only on three tiny spikes, making the vibrations as close to free as possible. For a more detailed description of our setup, see Ref. [22].

The rectangular block is made of fused quartz and has side lengths 14 mm, 25 mm, and 40 mm. The acoustic Q value is between 10^5 and 10^6 at a typical frequency of 500 kHz. Previous experiments [11,12] on single-crystal quartz blocks reported Q values of around 10^6 and utilized this high quality for measuring many eigenfrequencies.

III. DISPERSION RELATIONS AND WEYL LAW

In the bulk of our fused quartz block, transverse and longitudinal waves propagate independently with dispersion relations $k=2\pi f/c_t$ and $k=2\pi f/c_l$, where k is the wave number, f is the frequency, and c_t and c_l are the transverse and longitudinal wave speeds, respectively. An approximation to the Weyl law, i.e., the number of resonances,

$$N(f)\approx\frac{1}{c_l^3}\frac{(1+2\kappa^3)4\pi V}{3}f^3+\frac{1}{c_l^2}\frac{(3\kappa^4-3\kappa^2+2)\pi S}{4(\kappa^2-1)}f^2, \tag{1}$$

below frequency f, was calculated by Dupuis, Mazo, and Onsager [19], assuming free boundaries in two of the three spatial dimensions, and periodic boundary condition in the third. The same expression was reached by Safarov and Vassiliev [20] assuming, as far as we understand, free boundaries in all three spatial dimensions. Here, V is the volume of the system and S is the surface area. Reference [23] gives the values $c_t=3750$ m/s, $c_l=5894$ m/s, and Poisson's ratio $\nu=0.16$ for fused quartz. The ratio

$$\kappa=\frac{c_l}{c_t}=\sqrt{\frac{2(1-\nu)}{1-2\nu}} \tag{2}$$

depends only on ν and equals 1.57 with the values given above.

The resonances are, in general, mixtures of longitudinal and transverse waves that propagate independently inside the block but couple upon reflection at a boundary, where mode conversion takes place, see, e.g., Ref. [24] for details.

IV. ULTRASOUND TRANSMISSION SPECTRUM

An HP 3589A spectrum-network analyzer is used to measure the ultrasound transmission spectrum in the frequency range between 0 kHz and 885 kHz. The entire spectrum was measured three times with different locations of the block on the transducers. Using this method, resonance peaks that are hardly detectable in one spectrum are easily seen in the two other spectra. These measurements were carried out at a temperature of 35 °C. A section of the spectrum, from 600 kHz to 885 kHz, was then remeasured at a temperature of 40 °C. Two different positions of the block on the transducers was used to avoid missing levels, as explained above. Generally, no particular positions are selected, except that they must be different and we also try to avoid positions that are directly related to the symmetries of the block. A section of the transmission spectrum is plotted in Fig. 1 for the two different values of the temperature.

Notice that the temperature increase makes the resonance peaks shift upward in frequency. This comes about because the thermal expansion is negligible for fused quartz compared to the $d\nu/dT$ and dc_t/dT, that are both positive, see Eqs. (3) and (4).

All resonance peaks are fitted with a so-called skew Lorentzian [25] using interactive software developed in the programming language IDL. The fit parameters include the eigenfrequency and the width.

V. STAIRCASE FUNCTION

We find 2338 resonances in the frequency range from 0 kHz to 885 kHz. This number must be compared to the Weyl law, given in Eq. (1), which gives 2333. In Fig. 2 we show the measured staircase function along with the Weyl law Eq. (1). The agreement is striking, considering that Eq. (1) is an approximation that includes only the two leading terms. Looking at the difference between the measured staircase and the approximate Weyl curve (see inset to Fig. 2), which we call the fluctuations, it is clear that some systematic effect is present. The fluctuations cross zero only a few times in the entire frequency range. Nevertheless, the overall agreement is surprisingly good. To comment on the possibility of missing levels, we stress that two methods were applied to ensure correct level counting. First, several spectra were measured

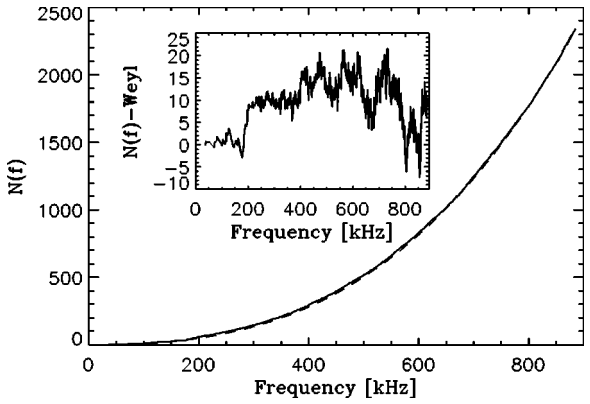

FIG. 2. The measured staircase function (solid step curve) compared to the Weyl law, Eq. (1) (dashed curve). Inset: The difference between the measured staircase function and the Weyl law.

in the entire frequency range for different transducer positions, and, second, a temperature perturbation was applied at the high frequencies, where the level density is higher, to split any accidental degeneracies or near degeneracies. We believe that no single level was missed. We note that Ref. [10] presents a similar comparison for an experiment with a block of aluminum, but the agreement is poor.

The Weyl curve, and hence the fluctuations, depends on the elastic constants used. In Fig. 2, we have used the values given above. Fitting the Weyl curve to the measured staircase gives smaller fluctuations, but unrealistic results for the elastic constants. The value for Poisson's ratio comes out negative which is unthinkable for fused quartz at room temperature. We also tried to include a linear term in the fit, but this only makes Poisson's ratio more negative. Including both a linear term and a constant gives $\nu=0.31$ which is equally unthinkable. We conclude that the unknown coefficients of any terms of order less than 2 depend on the two elastic constants, and therefore cannot be treated as free parameters. Were all terms of the Weyl law exactly known, one should in principle be able to determine the elastic constants with great precision by fitting the Weyl law to the experimental staircase.

VI. SPECTRAL FLUCTUATION STATISTICS

We now study the spectral fluctuation statistics. In Fig. 3 we present the spacing distribution and the $\Delta_3(L)$, calculated for the 2338 measured resonances of the fused quartz block. The eigenfrequency spectrum is unfolded with a polynomial of degree three, fitted to the measured staircase. Using instead the Weyl curve of Fig. 2 for the unfolding makes no visible change to the results shown in Fig. 3. It is clear that the data follow the "8-GOE" (Gaussian orthogonal ensemble) curve for the spacing distribution and for the $\Delta_3(L)$ up to $L=20$. The 8-GOE curve corresponds to a superposition of eight independent spectra, each with fluctuation properties of the GOE. This is to be expected, since the rectangular block has symmetry D_{2h} with eight nondegenerate classes. To our knowledge this is an experimental result that successfully identifies the precise number of irreducible representations directly from the spectral statistics for such a high degree of symmetry.

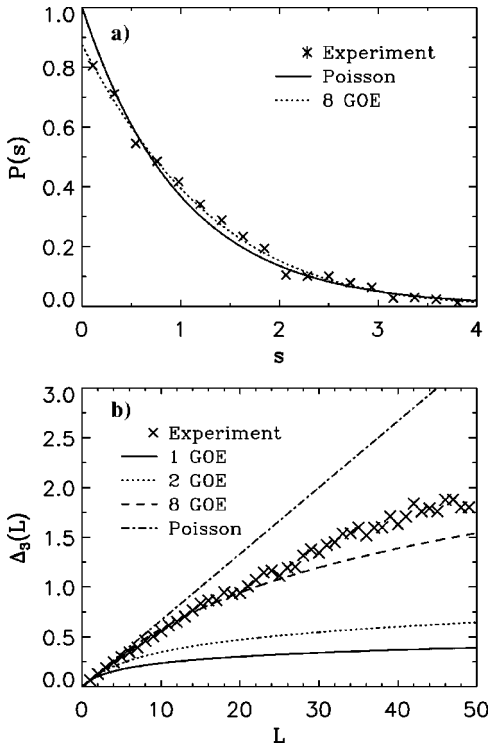

FIG. 3. The nearest neighbor spacing distribution (a) and the $\Delta_3(L)$ (b) calculated for the 2338 measured resonances of the rectangular fused quartz block. The curves labeled "2 GOE" and "8 GOE" correspond to a superposition of two and eight independent GOE spectra, respectively.

At $L>20$ the experimental $\Delta_3(L)$ lies systematically above the 8-GOE curve. As we shall see in the following, the block does allow the existence of bouncing-ball-like modes, that are not influenced by mode conversion. Although such resonances are too few in number to make a difference for the short range fluctuation statistics, it is very likely that they do influence the long range statistics. Indeed, the contribution to the spectral rigidity of a family of neutral periodic orbits in the stadium billiard was investigated in Ref. [27], and Fig. 7 of that paper shows that the correction to the $\Delta_3(L)$ is less than 0.08 for $L<20$, then grows to about 0.4 at $L=50$. A correction of similar size for our system would explain the observed deviation.

In the light of these findings, it is reasonable to comment on the results presented in Ref. [10] on spectral statistics of acoustic resonances in aluminum blocks. There it was demonstrated that for the rectangular block the statistics were Poissonian. It was mentioned that this could be a result of the high degree of symmetry, i.e., so many independent spectra contribute that their individual properties would not be seen because their total fluctuations are indistinguishable from Poissonian when the study includes only a few hundred levels. We can now see that this is certainly the explanation, and each of these spectra, if one could be extracted and studied on its own, must display GOE statistics due to mode conversion. The study of Ref. [10] was then really a study of sym-

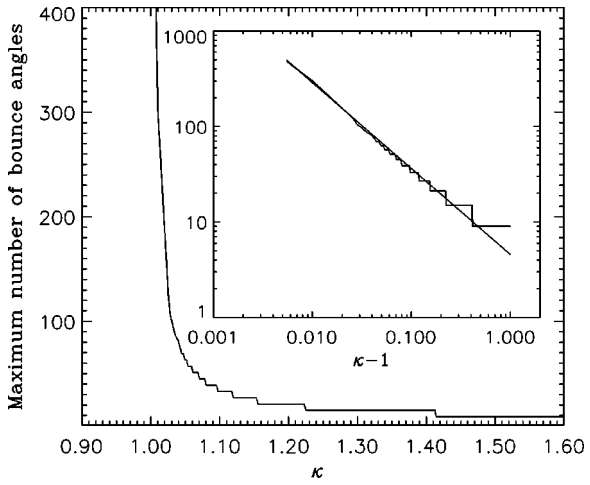

FIG. 4. Maximum number of bounce angles accessible to the particle as a function of κ in a simulation of the classical three-dimensional rectangular billiard with ray splitting. Inset: Same quantity shown as function of $\kappa-1$ in a $\log_{10}-\log_{10}$ plot along with a straight line fitted by eye.

metry breaking, going from many symmetries to no symmetries. We also note that our system shares the property of GOE-type fluctuation statistics despite nonergodic classical dynamics with the class of pseudointegrable systems, see, e.g., Ref. [28]. We expect this to hold as a general rule for the entire class of regular billiards with mode conversion.

Although the spectral fluctuation properties indicate chaotic behavior, it is understood that the rectangular billiard is not classically chaotic, even in the presence of ray splitting. In Ref. [26] it is found for the square billiard that only three momentum directions come into play if $\kappa \geqslant \sqrt{2} \approx 1.41$, and even for $\kappa < \sqrt{2}$ only a finite number of momentum directions are produced.

It is only in the limit $\kappa \rightarrow 1^+$ that more than a finite number of momentum directions can be reached. In a numerical calculation of ray dynamics with ray splitting in our three-dimensional rectangular billiard, we find that a similar picture emerges. We count the number of different bounce angles that are produced after a single launch and find the maximum of this number when launching rays in a 60×60 grid of angle space. In Fig. 4 we plot this maximum number of bounces as a function of κ. It is clear from this plot that for $\kappa > \sqrt{2}$ maximally 9 different bounce angles can be produced from a single initial condition. In principle, the curve has an infinite number of such transition points, always restricting the number of accessible bounce angles by 6 at each transition as κ increases, and with the last transition taking place at $\kappa = \sqrt{2}$. The exact values of κ where these transitions take place are unknown to us, except for the one at $\kappa = \sqrt{2}$ mentioned above. Numerically, we find that the first four transitions take place at $\kappa = 1.413$, 1.224, 1.154, and 1.119. We find that the curve can be estimated as $4.57(\kappa - 1)^{-0.9}$, see the inset to Fig. 4.

The numerical procedure used in the calculations is as in Ref. [15]. To generalize the numerical calculations in Ref. [15] to three dimensions, one must keep track of the polarization of the transverse wave, since in three dimensions it is not guaranteed to lie in the plane of incidence. We note, however, that since we are not interested in particular orbits or in the rate at which new bounce angles are produced, the actual conversion probability used has no influence on the results presented here, as long as it remains nonzero. We have therefore used a constant transition probability of 0.5, independent of the incidence angle. This choice has the additional advantage of speeding up the calculations, because the production of new angles is slow when the transition probabilities are small. Above the critical angle, given by $\sin(\theta_c) = 1/\kappa$, an incoming transverse wave cannot mode convert, and the transition probability in our calculation is set to zero.

For our fused quartz block, $\kappa \approx 1.57$, and the system is certainly not classically chaotic. Even so, the spectral fluctuations are well described by the GOE, in general agreement with the numerical work in Ref. [15], where it is found that mode conversion enhances chaoticity. Interestingly, it is found in Ref. [26] for the square billiard that the exponential proliferation of orbits, which is expected for $\kappa < \sqrt{2}$, persists at $\kappa \approx \sqrt{2}$, signifying the presence of topological chaos.

VII. MODE MIXING AND SPECIAL STATES

We may think of mode conversion as a symmetry-breaking mechanism that acts to mix transverse and longitudinal wave motion. These obey different dispersion relations, and their wavelengths change by different amounts in response to a change of temperature. In our experiments, this translates into shifts in eigenfrequency, which we can measure. That effect can be used to investigate to which degree a particular mode behaves as a transverse or a longitudinal mode. Differentiating the dispersion relations with respect to the temperature, we see that

$$\frac{df_t}{f_t} = \left(-\sigma + \frac{1}{c_t}\frac{dc_t}{dT} \right) dT \approx \frac{1}{c_t}\frac{dc_t}{dT} dT, \tag{3}$$

where T is temperature and σ is the thermal expansion coefficient. For fused quartz, σ can be ignored. Similarly, for longitudinal waves

$$\frac{df_l}{f_l} \approx \frac{1}{c_l}\frac{dc_l}{dT} dT = \left(\frac{1}{c_t}\frac{dc_t}{dT} + \frac{\kappa^2 - 1}{2\kappa(1-\nu)}\frac{d\nu}{dT} \right) dT, \tag{4}$$

and we note the additional term, proportional to $d\nu/dT$, compared to Eq. (3).

It was described in Sec. IV that we measured the 600–885 kHz section of the transmission spectrum at 35 °C and at 40 °C. This section contains 1512 resonance peaks. In Fig. 5 we show the resulting shift in eigenfrequency, normalized to the frequency as suggested in Eqs. (3) and (4). Since in this paper df/f serves merely as a label, for convenience we leave out a factor of 10^{-3} whenever we give numbers for df/f. The data points fall between a lower limit of about 0.36 and an upper limit of about 0.55, with a densely populated region closer to the lower limit.

We now study the distribution of df/f, see Fig. 6. To interpret the result, let us first consider what we would find if

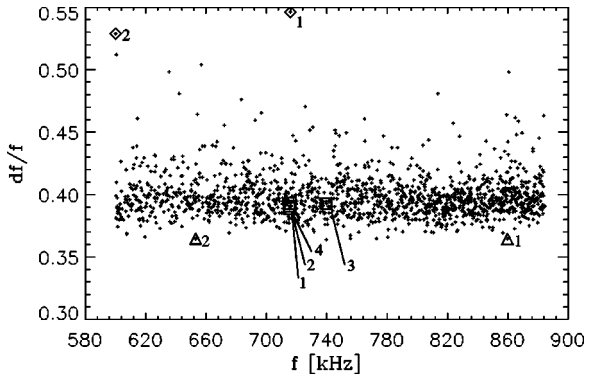

FIG. 5. Normalized eigenfrequency shift as a function of frequency for a temperature increase of 5 °C from 35 °C to 40 °C. Each "+" represents an eigenfrequency. For the eight data points marked with additional symbols ($\triangle, \square, \diamond$) we also measured the corresponding standing wave pattern, see Fig. 7.

mode conversion was not present. In that case, we would expect two δ-like peaks, one at df_t/f_t coming from the transverse modes, and one at df_l/f_l coming from the longitudinal modes. What we observe is that these δ-like peaks vanish as the symmetry is destroyed by mode conversion, producing instead a large peak of mixed modes. Very few data points remain where the δ-like peaks would have been. These few points are special resonances in the sense that they are protected from mode conversion and therefore do not participate in the mixing. In the following section we take a closer look at some of these special resonances. From Ref. [5] we have the estimates $df_t/f_t=0.37$ and $d\nu/dT=3.696\times10^{-5}\,°\mathrm{C}^{-1}$. Inserting these values into Eq. (4), we get $df_l/f_l=0.53$. We have not been able to find values for dc_t/dT and $d\nu/dT$ for fused quartz in the literature, and therefore cannot directly check these numbers.

It is of interest to compare Fig. 6 to Fig. 5 in Ref. [5], where the distribution of df/f for the rectangular plate is presented, and we have included that result in the inset to Fig. 6. For the rectangular plate it was found that small but significant peaks remained in the distribution, making up

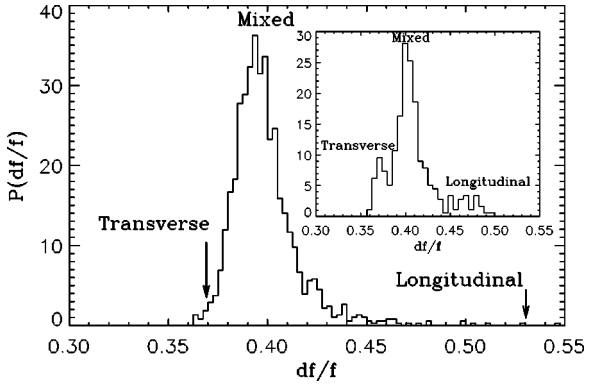

FIG. 6. Distribution of normalized frequency shift corresponding to a temperature increase of 5 °C. Arrows indicate where purely transverse and purely longitudinal resonances would contribute to the distribution. Inset: Corresponding result in two dimensions, i.e., for the rectangular plate.

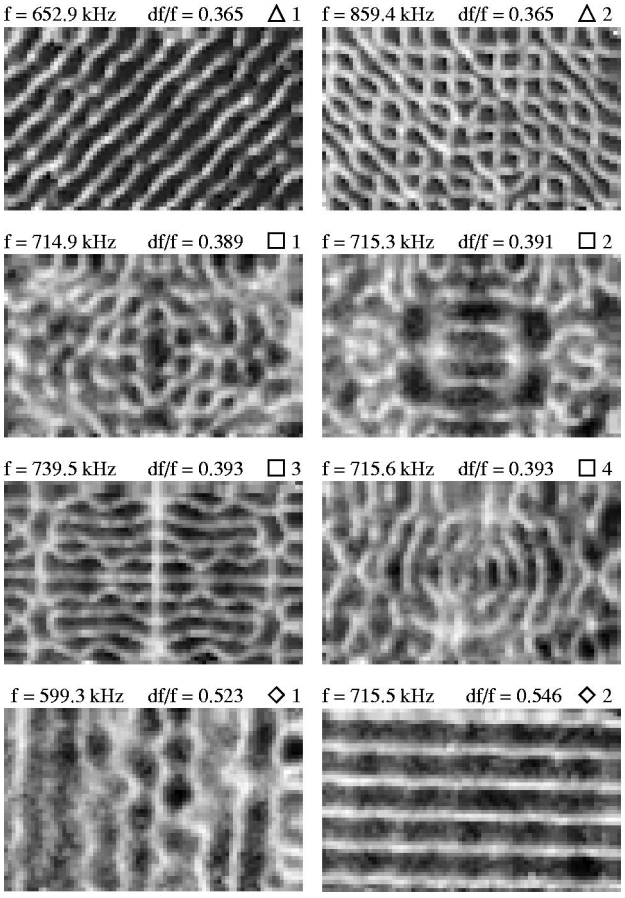

FIG. 7. Gray-scale plots of eight measured standing wave patterns. The gray scale is chosen logarithmic because this enhances contrast. The plots are ordered according to increasing value of the normalized frequency shift, df/f, and carry the same labels ($\triangle, \square, \diamond$) as in Fig. 5. Note that going from top left plot to lower right plot, one moves from transverse ($\triangle$), through mixed ($\square$), into longitudinal ($\diamond$), modes.

about 20% of the modes. For the block there are no such peaks, and the corresponding number is about 1%. We thus find that the mixing brought about by mode conversion is much stronger in the three-dimensional system than in the two-dimensional system. We are at present unaware of a general argument that can explain this remarkable difference.

Except for the special states, the symmetry-breaking scenario closely resembles the results obtained in Refs. [29,30] in a random matrix model for symmetry breaking. There, a so-called asymmetry number is defined, which measures to what extent an eigenvector belongs to one or the other of two, originally uncoupled, subspaces. Here, the normalized frequency shift plays the role of the asymmetry number. Moreover, it is a property of the above-mentioned model that the mean asymmetry number is conserved as the symmetry is broken, and equals the weighted average of the asymmetry number for the individual subspaces when the symmetry is good. Denoting by ρ_t and ρ_l the density of states for transverse and longitudinal modes, respectively, we find $\rho_t df_t/f_t+\rho_l df_l/f_l=0.402$, since $\rho_t/\rho_l=\kappa^3=3.88$. In comparison, the mean value of the distribution plotted in Fig. 6 is 0.399. The nice agreement indicates that our interpretation of Fig. 6 is correct.

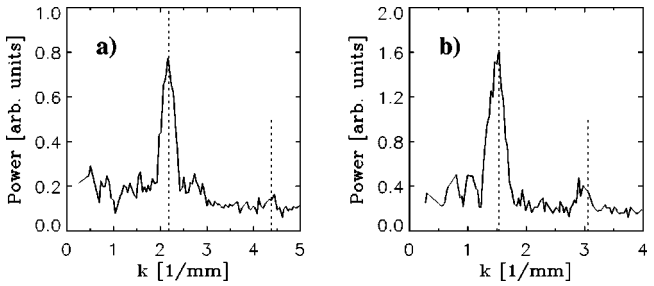

FIG. 8. Average FFT of "diagonal" sections of the standing wave pattern labeled "△1" (a), and of vertical sections of the standing wave pattern labeled "◇2" (b). A long dashed line is placed at twice the wave number of transverse and longitudinal wave motion, respectively. The shorter dashed lines indicate twice that value.

VIII. STANDING WAVE PATTERNS

Using a scanner we can measure standing wave patterns on one face of the rectangular block. The experimental technique used is presented in Ref. [22], which was designed for measurements on plates, but works well for any flat surface.

The method is to sweep the resonance peak in question for every point in a predefined grid on the surface. Roughly, one must then wait for two resonance lifetimes in order to obtain the vibration amplitude in one point, and the total measurement time is about 1 day for a scan of resolution 0.5×0.5 mm. This should not be considered a high-resolution scan, but it is good enough that we can interpret the measured standing wave patterns.

Based on the results presented in the preceding section, a number of resonance peaks were selected for such a measurement of the standing wave pattern. The purpose is to verify directly our finding in the preceding section, in particular that pure modes exist, although they are rare. We want to emphasize that the displacement field is a vector field in all three spatial dimensions. In our experiments the vibration is measured using a piezoelectric component with which we essentially measure an amplitude and a phase. For flexural modes of thin plates, we are confident that this amplitude is proportional to the actual vibration amplitude of the plate, see Ref. [22]. For resonances of the fused quartz block, the measured amplitude is some unknown function of the full displacement field. Nevertheless, it is possible to extract valuable information from the measured standing wave patterns. In Fig. 7 we show gray-scale plots of eight measured standing waves patterns. The first thing to notice about these standing wave patterns is how some modes seem very ordered whereas others look more irregular. Ordering the modes with respect to increasing df/f reveals a picture which is in perfect agreement with what we have found in the preceding section of this paper: The modes of smallest df/f, labeled "△," look regular because they belong to the special transverse resonances that are protected from mode conversion and therefore do not take part in the mixing. The modes of intermediate df/f, labeled "□," look complicated because they are mixtures of transverse and longitudinal wave motion. Finally, modes of high df/f, labeled "◇" are again ordered since they belong to the special longitudinal resonances.

Two of the measured standing wave patterns stand out as clean bouncing-ball modes, namely, the ones labeled "△1" and "◇2." In this case, we can compare the wave numbers to the dispersion relations to check if these are really transverse and longitudinal, respectively. In Fig. 8 we compare the wave numbers coming from the dispersion relations to the experiment, using fast Fourier transform (FFT). To calculate the wave numbers, we insert the resonance frequencies, given in Fig. 7, into the relevant dispersion relation. For longitudinal wave motion at 715.6 kHz, we find $k=2\pi f/c_l = 0.76\ \mathrm{mm}^{-1}$. Since the standing wave patterns represent the absolute value of the amplitude, the basic length scale is half the wavelength, corresponding to twice the wave number, i.e., $1.53\ \mathrm{mm}^{-1}$. Similarly, for transverse wave motion at 652.9 kHz, we expect $2.19\ \mathrm{mm}^{-1}$. In both cases, Fig. 8 shows that there is a large peak at the expected wave number. Although most modes are mixed, we have now seen directly that bouncing-ball-like modes are present, and that these are of either transverse or longitudinal character.

IX. DISCUSSION AND CONCLUSION

In Ref. [15], it is conjectured that one can expect GOE-type fluctuations for a much wider range of systems when mode conversion is present. Along with the results for the rectangular plate [5], the present study shows that an entire class of systems, the regular ray-splitting billiards, or rather, regular billiards with mode conversion, that were not considered before, also possess chaotic spectral fluctuations. It is our impression that the wave chaos in these classic elastodynamical systems has not previously been recognized and much theoretical work is needed to fully understand such systems. Experimental work on "statistical elastodynamics," as presented here and in Refs. [5,31], should serve to bring this to the attention of theoretical physicists.

We do not know of any numerical method that can reliably calculate several thousand eigenfrequencies for any of the two regular systems studied so far. It would therefore be difficult to calculate significant fluctuation statistics, and hence reveal the apparent wave chaos, by numerical means. Nevertheless, it is possible to calculate a few eigenfunctions at sufficiently high level number, which could answer interesting questions relating to the chaoticity of the standing waves. One could study the distribution and spatial correlation of intensity for the longitudinal part and the transverse part of an eigenfunction separately. The same information would be difficult to reach experimentally.

To summarize, we have measured acoustic transmission spectra and standing wave patterns of a rectangular block of fused quartz. We compare the measured staircase function to the approximate Weyl formula and find impressive agreement. The main focus of our work is to understand the influence of mode conversion in a regular, three-dimensional system. Using numerical simulation we confirm that the classical rectangular three-dimensional ray-splitting billiard is not chaotic. Nevertheless, the spectral fluctuation statistics of the 2338 measured eigenfrequencies follow the statistics

of eight superposed GOE spectra. The agreement is perfect at short range and shows a deviation at longer range which must be expected for systems with bouncing-ball-like modes. We confirm directly that such modes are present in our system, first by studying the distribution of normalized frequency shifts that arise from heating the block by 5 °C. This shows that almost all resonances are mixed by the mode conversion, except a few special resonances that remain either transverse or longitudinal. Second, by looking at standing wave patterns for these special resonances, measured on one face of the block. We find that the special modes display a high degree of order and we can directly measure the wave number for a transverse and a longitudinal mode, which agrees perfectly with the corresponding dispersion relation.

Our work shows that regular systems are interesting when mode conversion is present.

ACKNOWLEDGMENTS

The authors are grateful to Thiago N. Nogueira for technical assistance and to Predrag Cvitanović, Niels Søndergaard, Gregor Tanner, Thomas Guhr, Andrew D. Jackson, and Anders Andersen for valuable suggestions and discussions. K.S. gratefully acknowledges the hospitality of USP and the financial support from FAPESP.

[1] E. Bogomolny and E. Hugues, Phys. Rev. E **57**, 5404 (1998).
[2] P. Bertelsen, C. Ellegaard, and E. Hugues, Eur. Phys. J. B **15**, 87 (2000).
[3] P. Cvitanović, N. Søndergaard, and A. Wirzba, e-print nlin.CD/0108053.
[4] N. Søndergaard and G. Tanner (unpublished).
[5] K. Schaadt, G. Simon, and C. Ellegaard, Phys. Scr., T **T90**, 231 (2001).
[6] N. Søndergaard and G. Tanner (private communication).
[7] O. Bohigas, M.J. Giannoni, and C. Schmit, Phys. Rev. Lett. **52**, 1 (1984).
[8] B.D. Simons and B.L. Altshuler, Phys. Rev. Lett. **70**, 4063 (1993).
[9] R.L. Weaver, J. Acoust. Soc. Am. **85**, 1005 (1989).
[10] C. Ellegaard *et al.*, Phys. Rev. Lett. **75**, 1546 (1995).
[11] C. Ellegaard *et al.*, Phys. Rev. Lett. **77**, 4918 (1996).
[12] P. Bertelsen *et al.*, Phys. Rev. Lett. **83**, 2171 (1999).
[13] K. Schaadt and A. Kudrolli, Phys. Rev. E **60**, R3479 (1999).
[14] T. Guhr, A. Müller-Groeling, and H.A. Weidenmüller, Phys. Rep. **299**, 189 (1998).
[15] L. Couchman, E. Ott, and T.M. Antonsen, Jr., Phys. Rev. A **46**, 6193 (1992).
[16] Y. Hlushchuk *et al.*, Phys. Rev. E **61**, 366 (1999).
[17] N. Savytskyy *et al.*, Phys. Rev. E **64**, 036211 (2001).
[18] R. Schäfer *et al.*, Found. Phys. **31**, 475 (2000).
[19] M. Dupuis, R. Mazo, and L. Onsager, J. Chem. Phys. **33**, 1452 (1960).
[20] Y. Safarov and D. Vassiliev, in *Spectral Theory of Operators*, edited by S. G. Gindikin, AMS Translations Vol. 2, (American Mathematical Society, 1992), p. 150. See also http://www.mth.kcl.ac.uk/~ysafarov/Book/index.html
[21] S.W. McDonald and A.N. Kaufman, Phys. Rev. Lett. **42**, 1189 (1979).
[22] K. Schaadt, M.Sc. thesis, Niels Bohr Institute, Copenhagen, 1997. See also http://www.nbi.dk/~schaadt/speciale/speciale.ps.gz
[23] *CRC Handbook of Chemistry and Physics*, 76th ed., edited by R. C. Weast (CRC, Boca Raton, 1996).
[24] K. F. Graff, *Wave Motion in Elastic Solids* (Dover, New York, 1975).
[25] H. Alt *et al.*, Nucl. Phys. A **560**, 293 (1993).
[26] D. Biswas, Phys. Rev. E **54**, 1232 (1996).
[27] M. Sieber *et al.*, J. Phys. A **26**, 6217 (1992).
[28] T. Cheon and T.D. Cohen, Phys. Rev. Lett. **62**, 2769 (1989).
[29] A. Andersen, *Topics in Random Matrix Theory*, M. Sc. thesis, Niels Bohr Institute, Copenhagen, 1999. See also http://www.nbi.dk/~aanders/thesis.ps
[30] A. Andersen *et al.*, Phys. Rev. E **63**, 066204 (2001).
[31] K. Schaadt, Ph.D. thesis, Niels Bohr Institute, Copenhagen, 2001. See also http://www.nbi.dk/~schaadt/thesis.ps.gz